Temperature degradation of 2.3, 3.2 and 4.1 THz quantum cascade lasers

© D.A. Belov[1], A.V. Ikonnikov[1], S.S. Pushkarev[2], R.R. Galiev[2], D.S. Ponomarev[2], D.R. Khokhlov[1], D.V. Ushakov[3], A.A. Afonenko[3], S.V. Morozov[4], V.I. Gavrilenko[4], R.A. Khabibullin[2,5]

[1] Lomonosov Moscow State University (Department of Physics),
119991 Moscow, Russia
[2] Mokerov Institute of Ultra High Frequency Semiconductor Electronics of RAS,
117105 Moscow, Russia
[3] Belarusian State University,
220030 Minsk, Belarus
[4] Institute of Physics of Microstructures, Russian Academy of Sciences,
603950 Nizhny Novgorod, Russia
[5] Ioffe Institute,
194021 St. Petersburg, Russia

E-mail: belov.da17@physics.msu.ru

Received March 2, 2022
Revised March 25, 2022
Accepted March 25, 2022

In this work, we conduct research of spectral and power characteristics of quantum cascade lasers (QCLs) based on a GaAs/$Al_{0.15}Ga_{0.85}As$ active region emitting at 2.3 (A), 3.2 (B) and 4.1 (C) THz. The QCL devices had a double-metal Au waveguide and operated in pulsed mode with 1.5−9 μs pulses at 20 Hz repetition rate. Using the integral output power curves measured with different pulse durations, we consider the potential mechanisms of QCL temperature degradation using Arrhenius plots. Moreover, we present the spectra of the lasers measured at fixed operating points for devices A, C and with current scanning for device B in a wide temperature range from 5 to 120 K. We hope that our results will prove useful for research concerning QCL maximum operating temperatures.

Keywords: quantum cascade laser, terahertz range, quantum well, molecular beam epitaxy, activation energy, temperature degradation.

DOI: 10.21883/SC.2022.07.54656.19

1. Introduction

Quantum-cascade lasers (QCL) are currently one of the most promising types of sources of terahertz (THz) radiation [1,2]. The compactness of such lasers, relatively high output power, and the ability to freely adjust the generation frequency in the $\sim 1-5$ THz range by changing the thickness of the heterostructure layers make them very attractive for many applications [3]. The main obstacle standing in the way of the widespread use of such lasers is that THz radiation is generated only at low temperatures, which require the use of expensive coolers. The development of band designs of the active region and low-loss waveguides made it possible to demonstrate in 2020 THz QCLs operating at a temperature of 250 K (about -23°C) with cooling on single-stage Peltier element [4]. The operation of a THz QCL at room temperature has not yet been demonstrated.

Necessary condition for the creation of THz QCLs capable of operating at $T = 300$ K is the understanding of mechanisms of thermal damping for the generation of such lasers at high temperatures. At the same time, experience has shown that even the study of these mechanisms is not easy performance due to a number of circumstances. First, in the lasers under consideration with a resonant-phonon design, on the basis of which THz QCLs with record temperatures [3–5] were demonstrated, there are several different factors that affect the thermal damping of generation, and their contribution to the resulting effect is not clear in advance. Moreover, attempts to create lasers with a design aimed at suppressing one or another mechanism of thermal damping of generation do not lead to significant increase in the operating temperature, and sometimes even lead to its decrease [6]. As a result, a clear separation of the contributions of the various mechanisms is currently not possible. Secondly, the experimental study of the corresponding mechanisms is hampered by the fact that the temperature of the electronic subsystem differs significantly from the heat removal temperature at $T \lesssim 100$ K [7–9]. Thirdly, all known studies of the thermal attenuation of the generation of pulsed lasers, as well as studies of lasers with record operating temperatures, were carried out at short pulse durations i.e. less than 300 ns. Such durations practically exclude the effect of Joule heating on the operation of lasers, but at the same time they significantly limit their maximum output power. The most promising for practical problems operating mode of THz QCLs with long pulse durations ($> 1\,\mu$s) remains poorly studied.

Nevertheless, the method was proposed in the work [10] that makes it possible to estimate the contribution of one of the mechanisms of thermal damping of generation, —

temperature activation of the emission of longitudinal optical (LO) phonons „by hot“ electrons from the upper laser level. This process is characterized by the electron activation energy E_a at thermal excitation, leading to nonradiative transition to the lower laser level with the emission of a LO-phonon: $\hbar\omega_{LO} = E_a + \hbar\omega$, where $\hbar\omega$ is the laser radiation energy (the distance between the upper and lower laser levels). The decisive contribution of the described mechanism should be evidenced by the value of the activation energy, which can be determined using the Arrhenius plot of the normalized laser output power versus temperature when considering the high-temperature region (~ 100 K), where the electron temperature is close to the lattice temperature.

In the present work, this method was applied to analyze the temperature dependences of the power characteristics of a THz QCL with a resonant-phonon design, measured at sufficiently long pulse durations of $1.5-9\,\mu$s.

2. Experimental samples and measurement procedure

In the work, QCLs (№ 22119, 42233*R, 25231R), fabricated at IMSE RAS based on active module of three and four GaAs/$Al_{0.15}Ga_{0.85}$As quantum wells with a resonant-phonon design, emitting at frequencies of 2.3, 3.2, and 4.1 THz were studied, (hereinafter, these lasers will be designated A, B, and C, respectively). The QCLs under study had a double metallic waveguide Au–Au. The Fabry–Perot resonator was formed by cleaving off laser strips $100\,\mu$m wide and 1 to 2 mm long. The preparing method is described in detail in [11,12].

In the course of the work, a series of measurements was made of the dependences of the output power on the operating current ($L-I$) and QCL spectra with a resolution of $0.2\,\text{cm}^{-1}$ (6 GHz) in wide temperature range. The lasers were powered in a pulsed mode using electronic switch that generated voltage pulses of specified duration τ_L, repetition frequency f_L, and amplitude U_L, as well as allowing control of the current and tension. Measurements of $L-I$-characteristics were carried out at pulse durations $\tau_L = 1.5-9\,\mu$s with repetition rate $f_L = 20$ Hz, in while the spectra were measured using the pulse duration $\tau_L = 5-15\,\mu$s and the repetition frequency $f_L = 1$ kHz. The QCLs were placed in an Oxford Optistat CF helium continuous-flow cryostat, which makes it possible to maintain the temperature from 4.2 to 300 K. The laser radiation was output through the polyethylene windows of the cryostat using the metal waveguide. During measuring the $L-I$-characteristics, the waveguide was connected to the input polyethylene window of an IRLabs silicon bolometer. Signal from the bolometer was fed to the input of a Stanford Research Systems SR250 gated integrator, which was used to determine the amplitude of the detected signal. During measuring the emission spectra, the waveguide was connected to the input port of the Fourier-spectrometer Bruker Vertex 70v, which made it possible to evacuate the optical path. Standard pyroelectric receiver with black polyethylene filter was used to detect THz radiation. Since, at the selected repetition frequency, the time constant of the receiver exceeds the repetition time of the radiation pulses, this mode of operation is equivalent to the continuous mode of the laser. This made it possible to use the spectrometer in the continuous scanning mode.

3. Results and discussion

In accordance with the procedure proposed in the work [10], to estimate the contribution of scattering by optical phonons to the temperature damping of laser generation, it is necessary to construct Arrhenius plots of the normalized output power versus temperature. In the case where specified contribution is decisive, the attenuation of the radiation power should have a thermoactivation nature, which manifests itself in the presence of a linear section on the Arrhenius plot in the region of high temperatures, where the electron temperature is close to the lattice temperature. The slope of the resulting straight line is characterized by the activation energy E_a. According to the theory, the sum E_a with a THz photon energy $\hbar\omega$ equal to the energy distance between the lower and upper laser levels should be close to the LO-phonon energy, which is $\hbar\omega_{LO} \approx 36.5$ meV in GaAs. The output power was determined from the extrema of the $L-I$ curves and normalized to the values obtained at $T = 5$ K.

Fig. 1–3 show the results of measurements of the radiative characteristics of studied QCLs in the temperature range from 5 to 120 K, including $L-I$-characteristics of lasers and Arrhenius plots constructed on their basis, as well as emission spectra of lasers (see inserts). For laser B, the studies were carried out at three different values of τ_L in order to establish the degree of influence of the nature of the pulsed power supply of QCLs on their temperature

The parameters of the studied THz QCLs: the generation frequency f and the corresponding photon energy $\hbar\omega$, the expected activation energy $E_{a(\text{theor})} = E_{LO} - \hbar\omega$ and obtained from the Arrhenius plot $E_{a(\text{exp})}$ for current pulse durations τ_L, maximum operating temperature $T_{\max}$

Laser	f, THz	$\hbar\omega$, meV	$E_{a(\text{theor})}$, meV	τ_L, μs	$E_{a(\text{exp})}$, meV	$T_{\max}$, K
A	2.3	9.5	27	9	12.4	80
B	3.2	13.2	23.3	1.5	28.5 23.0*	120
				4.5	23.5	
				9	17.8	
C	4.1	17.0	19.5	9	6.6	110

Note. * normalized at $\tau_L = 4.5\,\mu$s.

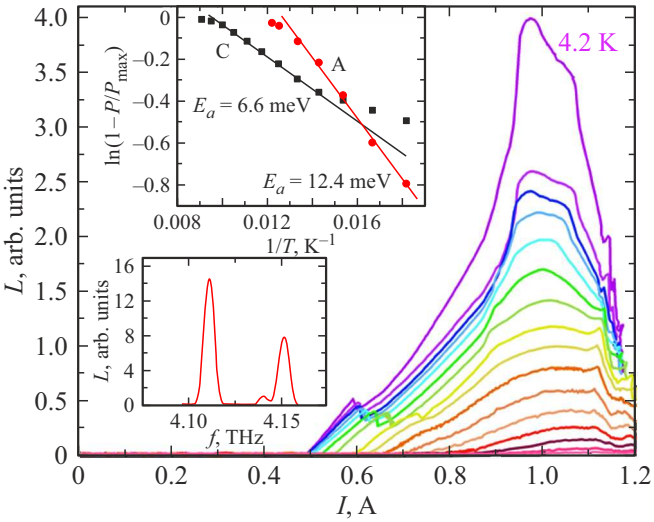

Figure 1. $L-I$-laser characteristics C measured at temperatures from 4.2 to 110 K with pulse parameters 9 μs/20 Hz The temperature increases from cold colors to warm ones. On inserts — Arrhenius plots for lasers A and C and the radiation spectrum of laser C at a temperature of 5 K, measured at current of 1.03 A with pulse parameters of 10 μs/1 kHz. (A color version of the figure is provided in the online version of the paper).

degradation. The values of the activation energies obtained and the main parameters of the studied THz QCLs are presented in the Table.

$L-I$-characteristics of lasers A and C were measured with pulse durations $\tau_L = 9\,\mu$s at a repetition rate $f_L = 20$ Hz in temperature ranges 5–80 and 4.2–110 K, respectively Fig. 1 shows the $L-I$- characteristic of the C laser, as well as the Arrhenius plots for the A and C lasers. The high-temperature sections of these graphs are characterized by the activation energies $E^A_{a(\exp)} = 12.4$ meV and $E^C_{a(\exp)} = 6.6$ meV, which in sum with the energies of the corresponding photons $\hbar\omega$ give 21.7 and 23.5 meV.

The specified summarized energies are $E_a + \hbar\omega$ for lasers A and W ith significantly less energy of the longitudinal optical phonon in GaAs ($\hbar\omega_{LO} \approx 36.5$ meV). Such a strong discrepancy can be explained by decrease in the effective duration of the radiation pulse due to heating of the QCL by the flowing current; this mechanism will be discussed in more detail below. In addition, the difference in energies for a low-frequency laser A can be related to the influence of alternative lasing damping mechanism associated with decrease in the time of maintaining the coherence of electron waves involved in resonant tunneling from the injector level to the upper laser level. A more precise definition of the role of various mechanisms in lasers with resonant-phonon design is a topic for further research.

$L-I$-characteristics of the B laser were measured at three different pulse durations τ_L: 1.5 μs (Fig. 2, *a*), 4.5 μs (Fig. 2, *b*) and 9 μs (Fig. 2, *c*) with repetition frequency $f_L = 20$ Hz in the temperature range 4.2–120 K. The non-monotonicity of the dependence $L-I$ is related to the effect „of jump“ generation modes [13] with the participation of the 3.8 THz mode, which appears at temperatures > 80 K in the region of high operating currents. This is evidenced by the radiation spectra of the B laser, measured at a temperature of 85 K and shown in the inset in Fig. 2, *a*. Since this mode exists only in a narrow temperature range, its influence was not taken into account in our consideration.

Figure 3 shows the Arrhenius plots for B laser over the entire temperature range for three pulse durations. The activation energies corresponding to the pulse durations 1.5, 4.5, and 9 μs are 28.5, 23.5, and 17.8 meV, which together with the photon energy gives the values 41.7, 36.7, and 31.0 meV. It is easy to see that the total energy obtained at intermediate pulse duration $\tau_L = 4.5\,\mu$s practically coincides with the *LO*-phonon energy, while for other pulse durations deviations are observed as to the greater, and to the smaller side. In the case of longer pulses, this behavior can be explained by the aforementioned decrease in the effective duration of the radiation pulse, which is related to the Joule heating of the laser during the current pulse. Such heating leads, first of all, to a certain decrease in the laser radiation frequency within a pulse due to a change in the effective refraction index of the active region [14,15]. Another effect is the decrease in radiation intensity with increasing temperature, and the longer the pulse duration, the more significant this effect manifests itself within single pulse. At sufficiently high temperatures, the current flowing through the QCL can heat it above the maximum operating temperature, which will lead to premature attenuation of the radiation pulse, and the actual power in the pulse will be noticeably lower than the nominal one. This is due to the fact that when measuring $L-I$-characteristics, we use the „slow“ bolometric receiver, whose time constant (~ 1 ms) is much greater than the duration of laser pulses. Because of this, the measured signal amplitude is proportional not only to the intensity of the laser radiation, but also to its duration. Accordingly, premature attenuation of the laser during the pulse will lead to decrease in the recorded signal value.

When analyzing the obtained $L-I$-dependences, it should also be taken into account that, since the activation mechanism of *LO*-phonon emission from the upper laser level described above refers to a nonradiative process that reduces total radiation intensity, then the construction of Arrhenius plots is advisable for the difference between the maximum (normalization) power $P_{\max}$ measured at low temperature (when the indicated nonradiative mechanism is absent) and the current power P, since it is this difference has the exponential temperature dependence.

Because of this, the slope of the linear section of the plot, and hence the activation energy, significantly depend on the value of the normalization power: if it increases, then the activation energy decreases, and the linear section becomes flatter, and vice versa. Accordingly, as the effective pulse duration decreases, the normalization power used in the calculations turns out to be greater than it should be for these pulses, which leads to decrease in the activation

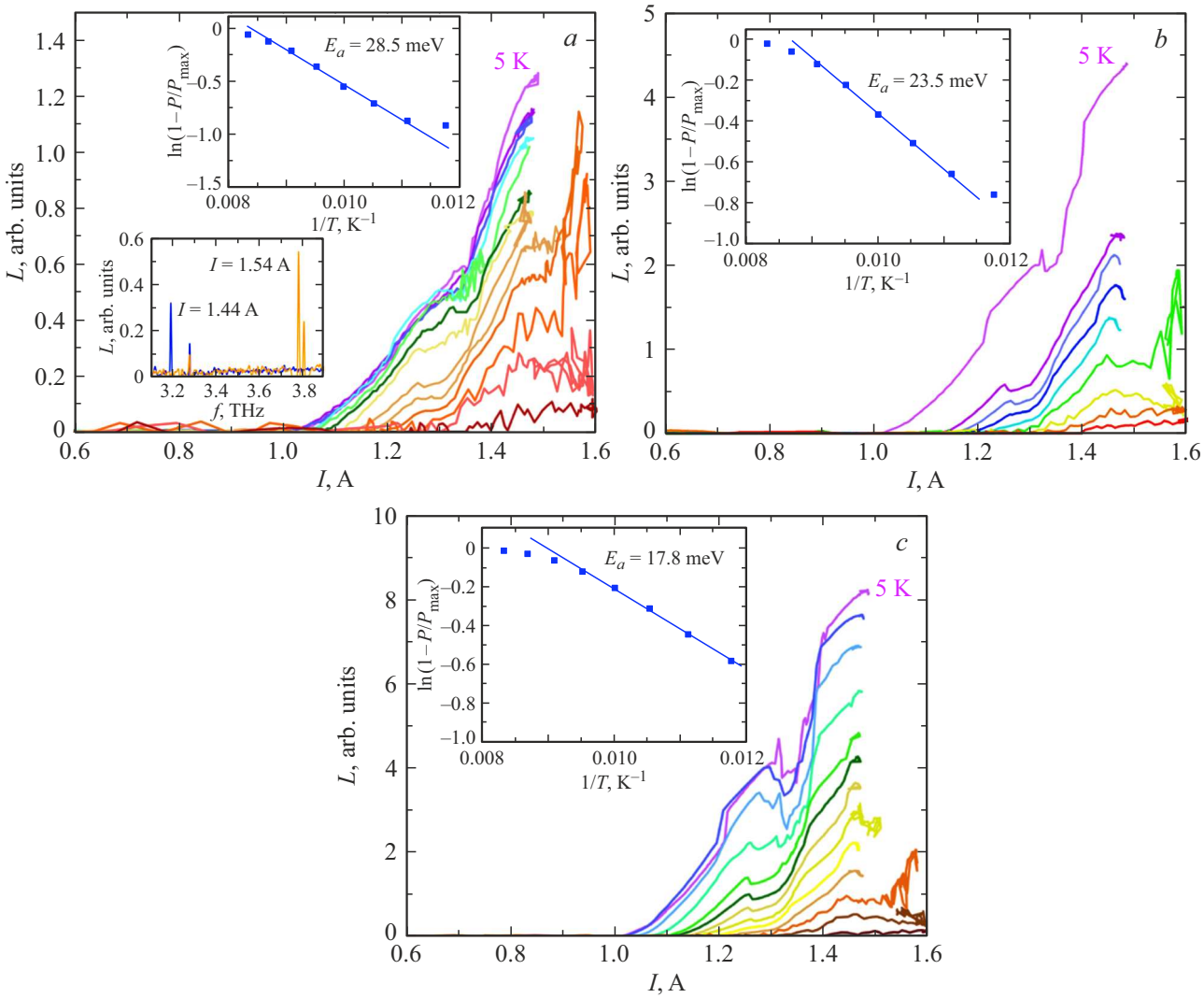

Figure 2. L–I-laser B characteristics measured at temperatures from 5 to 120 K. The temperature increases from cold colors to warm ones. The repetition frequency $f_L = 20$ Hz, pulse durations τ_L are: *a* — 1.5 μs, *b* — 4.5 μs, *c* — 9 μs. Inserts shows the Arrhenius plots based on the presented curves. Figure *a* also shows the emission spectra measured at $T = 85$ K with pulse parameters 5 μs/1 kHz at two current values: 1.44 and 1.54 A. At a higher current, there is a jump in the laser modes from 3.2 to 3.8 THz.

energy and the slope of the straight line compared to the values corresponding to the *LO*-phonon. Namely this behavior is demonstrated by the Arrhenius plot for all considered QCLs at $\tau_L = 9\,\mu$s. It should also be noted that starting from the temperature ~ 100 K the dependences L–I for the laser B at $\tau_L = 4.5\,\mu$s and $\tau_L = 9\,\mu$s are completely close. This observation can be explained by the fact that the effective pulse durations become $< 4.5\,\mu$s at the indicated temperatures. The same mechanism explains the difference from the linear dependence on the Arrhenius plots at high temperatures for all lasers i.e. the time during which the laser still emits is reduced, which leads to a drop in the amplitude of the measured signal. Similar effect was also observed by us for the temperature dependence of the power of a THz QCL with a generation frequency of 3.3 THz, measured at $\tau_L = 2\,\mu$s (see Fig. 6 in [16]).

In the case of shorter pulses, the temperature dependence of the output power can be explained by finite (and significant) rise time of the laser radiation pulse to the nominal value. Similar effect was observed, for example, in the work [17], in which frequency tuning of a THz QCL with a resonant-phonon design was studied during long (up to 50 μs) radiation pulses. In the work [17] oscilloscope record of the radiation pulse is given, from which it follows that the nominal power is reached in 4 μs. For the lasers studied in this work, this time is $t_{\text{rise}} \sim 1\,\mu$s, which can be related both to the features of the laser and to the finite rise time of the current pulse from the switch that feeds the QCL. Note that this time does not depend on the pulse length, as a result of which its „contribution“ to the measured power decreases with increasing pulse duration. When short pulses are used, t_{rise} forms a significant part of them, due to which the actual power in the pulse turns

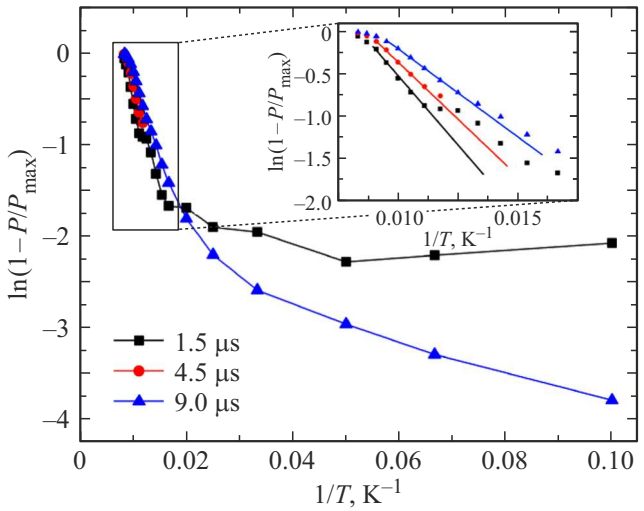

Figure 3. Arrhenius plots for laser B with three pulse durations τ_L: 1.5, 4.5 and 9 μs.

out to be less than the nominal one, and, just as before, does not correspond to normalization values. Following the reasoning given above, we find that the normalization power turns out to be less than it should be at zero value of t_{rise}. This entails increase in the activation energy and increase in the slope of the linear section, which we see on the Arrhenius plot for $\tau_L = 1.5\,\mu$s (Fig. 3). At the same time, at high temperatures, the influence of t_{rise} also decreases, since at constant current pulse amplitude, the radiation pulse amplitude decreases with temperature. This means that the nominal value of the radiation pulse power is reached earlier, and t_{rise} itself decreases with increasing temperature. To confirm these arguments, one can estimate the activation energy for the laser B at $\tau_L = 1.5\,\mu$s at small influence of t_{rise}. Using the value for $\tau_L = 4.5\,\mu$s, reduced by $4.5/1.5 = 3$ times as the normalization power, we obtain the value of the total energy equal to 36.2 meV, which is very close to the energy *LO*-phonon. Note that the values at $\tau_L = 9\,\mu$s are not suitable for such an assessment, because with such a pulse duration, Joule heating has a significant effect even at low temperatures. This can be verified by comparing the low-temperature sections of the Arrhenius plots for pulse durations $\tau_L = 1.5\,\mu$s and $\tau_L = 9\,\mu$s: the decline of the latter starts from the lowest temperatures, while at $\tau_L = 1.5\,\mu$s the power practically does not change up to $T \sim 65$ K.

The above results and reasoning indicate that the dominant mechanism of thermal damping of generation in the investigated THz QCLs with resonant-phonon design is the thermal activation of the emission of *LO*-phonons by „hot“ electrons from the upper laser level. The optimal pulse duration for such studies using our measuring system is $\tau_L \sim 4.5\,\mu$s, since such an injection mode, on the one hand, makes the laser less susceptible to Joule heating at low temperatures, and on the other hand makes it possible to observe the beginning of the temperature section, in which the indicated generation damping mechanism manifests itself.

4. Conclusion

In this work, the temperature dependences of the power and spectral characteristics of QCLs with a resonant-phonon design based on the GaAs/$Al_{0.15}Ga_{0.85}As$ active region emitting at frequencies of 2.3, 3.2, and 4.1 THz, were studied. The measured temperature dependences of the integral output power of the laser radiation were used to construct Arrhenius plots, which make it possible to consider possible mechanisms for the thermal damping of generation. The results obtained indicate that the dominant mechanism of lasing damping in the studied QCLs is the temperature activation of the emission of *LO*-phonons „by hot“ electrons from the upper laser level, which means that the procedure used can be applicable to operating modes with microsecond pulses.

Funding

The study was performed with the support of RSF grant No. 21-72-30020. D.A. Belov thanks the „BAZIS“ foundation for support (grant No. 21-2-9-45-1).

Conflict of interest

The authors declare that they have no conflict of interest.

References

[1] M.S. Vitiello, G. Scalari, B. Williams, P.D. Natale. Opt. Express, **23**, 5167 (2015).
[2] G. Liang, T. Liu, Q.J. Wang. IEEE J. Select. Top. Quant. Electron., **23**, 1200118 (2017).
[3] L. Bosco, M. Franckie, G. Scalari, M. Beck, A. Wacker, J. Faist. Appl. Phys. Lett., **115**, 010601 (2019).
[4] A. Khalatpour, A.K. Paulsen, C. Deimert, Z.R. Wasilewski, Q. Hu. Nature Photonics, **15**, 16 (2021).
[5] S. Fathololoumi, E. Dupont, C.W.I. Chan, Z.R. Wasilewski, S.R. Laframboise, D. Ban, A. Mátyás, C. Jirauschek, Q. Hu, H.C. Liu. Opt. Express, **20**, 3866 (2012).
[6] S. Khanal, L. Zhao, J. Reno, S. Kumar. J. Opt., **16**, 094001 (2014).
[7] H. Callebaut, S. Kumar, B.S. Williams, Q. Hu, J.L. Reno. Appl. Phys. Lett., **83**, 207 (2003).
[8] P. Slingerland, C. Baird, R.H. Giles. Semicond. Sci. Technol., **27**, 65009 (2012).
[9] M.S. Vitiello, G. Scamarcio, V. Spagnolo, B.S. Williams, S. Kumar, Q. Hu, J.L. Reno. Appl. Phys. Lett., **86**, 111115 (2005).
[10] A. Albo, Q. Hu. Appl. Phys. Lett., **106**, 131108 (2015).
[11] R.A. Khabibullin, N.V. Shchavruk, D.S. Ponomarev, D.V. Ushakov, A.A. Afonenko, K.V. Maremyanin, O.Yu. Volkov, V.V. Pavlovskiy, A.A. Dubinov. Opto-Electron. Rev., **27**, 329 (2019).

[12] R.A. Khabibullin, N.V. Shchavruk, A.Yu. Pavlov, D.S. Ponomarev, K.N. Tomosh, R.R. Galiev, P.P. Maltsev, A.E. Zhukov, G.E. Tsyrlin, F.I. Zubov, Zh.I. Alferov. FTP **50**, 1395 (2016) (in Russian).
[13] O.Yu. Volkov, I.N. Dyuzhikov, M.V. Logunov, S.A. Nikitov, V.V. Pavlovsky, N.V. Shchavruk, A.Yu. Pavlov, R.A. Khabibullin. Radiotekhnika i elektronika, **63**, 981 (2018) (in Russian).
[14] J.M. Hensley, J. Montoya, M.G. Allen, J. Xu, L. Mahler, A. Tredicucci, H.E. Beere, D.A. Ritchie. Opt. Express, **17** (22), 20476 (2009).
[15] A.A. Lastovkin, A.V. Ikonnikov, V.I. Gavrilenko, A.V. Antonov, Yu.G. Sadofiev. Izv. vuzov. Radiofizika, **54**, 676 (2011) (in Russian).
[16] R.A. Khabibullin, N.V. Shchavruk, D.S. Ponomarev, D.V. Ushakov, A.A. Afonenko, I.S. Vasilevsky, A.A. Zaitsev, A.I. Danilov, O.Yu. Volkov, V.V. Pavlovsky, K.V. Maremyanin, V.I. Gavrilenko. FTP, **52** (11), 1268 (2018) (in Russian).
[17] A.A. Lastovkin, A.V. Ikonnikov, A.V. Antonov, V.Ya. Aleshkin, V.I. Gavrilenko, Yu.G. Sadofiev. Pis'ma ZhTF, **42** (5), 15 (2016) (in Russian).